

PORTLLM: PERSONALIZING EVOLVING LARGE LANGUAGE MODELS WITH TRAINING-FREE AND PORTABLE MODEL PATCHES

Anonymous authors

Paper under double-blind review

ABSTRACT

As large language models (LLMs) increasingly shape the AI landscape, fine-tuning pretrained models has become more popular than in the pre-LLM era for achieving optimal performance in domain-specific tasks. However, pretrained LLMs such as ChatGPT are periodically evolved (*i.e.*, model parameters are frequently updated), making it challenging for downstream users with limited resources to keep up with fine-tuning the newest LLMs for their domain application. Even though fine-tuning costs have nowadays been reduced thanks to the innovations of parameter-efficient fine-tuning such as LoRA, not all downstream users have adequate computing for *frequent personalization*. Moreover, access to fine-tuning datasets, particularly in sensitive domains such as healthcare, could be time-restrictive, making it crucial to retain the knowledge encoded in earlier fine-tuned rounds for future adaptation. In this paper, we present PORTLLM, a training-free framework that (i) creates an initial lightweight model update patch to capture domain-specific knowledge, and (ii) allows a subsequent seamless plugging for the continual personalization of evolved LLM at minimal cost. Our extensive experiments cover **seven** representative datasets, from easier question-answering tasks {BoolQ, SST2} to harder reasoning tasks {WinoGrande, GSM8K}, and models including {Mistral-7B, Llama2, Llama3.1, and Gemma2}, validating the portability of our designed model patches and showcasing the effectiveness of our proposed framework. For instance, PORTLLM achieves comparable performance to LoRA fine-tuning with reductions of up to $12.2\times$ in GPU memory usage. Finally, we provide theoretical justifications to understand the portability of our model update patches, which offers new insights into the theoretical dimension of LLMs’ personalization.

1 INTRODUCTION

The rise of large pretrained language models has marked a significant shift in natural language processing (NLP), [particularly in their ability to adapt to specific domains and tasks](#). These models, such as GPT-4 (Achiam et al., 2023), have achieved state-of-the-art performance by leveraging vast amounts of pretraining data (Antoniades et al., 2024). [However, pretrained LLMs often require adaptation for specialized domains where context-specific knowledge is critical](#) (Wang et al., 2022a; Bommasani et al., 2021; Qiu et al., 2020). Hence, while pretraining [provides a strong foundation](#), *fine-tuning* (*e.g.*, *personalization*) is essential for specific domains. Fine-tuning bridges this gap by adapting pretrained models to specific tasks, enhancing their performance in domains such as healthcare, legal analysis, or scientific research (Min et al., 2021; Wei et al., 2021; Ouyang et al., 2022; Wang et al., 2022b; Liu et al., 2022; Raffel et al., 2020; Chen et al., 2024; Gao et al., 2024b). For instance, fine-tuned models can more effectively recognize domain-specific terminology, reason about complex relationships, and deliver more accurate and contextual appropriate responses.

Much effort has been devoted to developing fine-tuning methods. Traditionally, fine-tuning would normally involve updating all the parameters of a model. For example, in the case of Mistral 7B (Jiang et al., 2023), it would involve updating all 7 billion parameters. Typically LLMs have billions of parameters, and so this process poses significant challenges in computational and memory requirements. To alleviate these constraints, many Parameter Efficient Fine-Tuning (PEFT)

054 methods (Houlsby et al., 2019) have been proposed. One popular method is Low-Rank Adaptation
 055 (LoRA) (Hu et al., 2021), which aims to estimate an updated matrix ΔW using the product of two
 056 low-rank matrices A and B . However, although LoRA lowers the training complexity, it still re-
 057 quires fine-tuning a large number of trainable parameters to reach a satisfactory performance. For
 058 example, LoRA fine-tuning Llama 2 13B (Touvron et al., 2023) variant would require up to eight
 059 A6000 GPUs with 48 GB VRAM each, for a very small batch size, hence imposing a considerable
 060 memory and computational burden.

061 Furthermore, as cloud-hosted LLMs like ChatGPT (OpenAI, 2022) and Gemini (Team et al., 2023)
 062 undergo periodic (bi-annually or shorter) updates with newer data, their improved performance often
 063 renders previous versions outdated. For downstream users who have already invested in fine-tuning
 064 these models for domain-specific tasks, repeatedly fine-tuning or performing personalization at ev-
 065 ery new update is highly impractical, as the process is not only computationally expensive but also
 066 time-consuming.

067 Beyond the computational and logistical hurdles, continual updates present another challenge for the
 068 downstream user: the lack of availability of the fine-tuning dataset. In domains such as healthcare
 069 or finance, data access is regulated by privacy laws and potentially time-sensitive. For example,
 070 fine-tuning medical models on patient data requires strict adherence to ethical and legal guidelines,
 071 making it difficult to repeatedly fine-tune with every model update. As a result, repeatedly fine-
 072 tuning models on newer LLM releases is not a viable long-term strategy for many users, hindering
 073 the downstream users from harnessing the performance gains from the evolving nature of LLMs. In
 074 response to these challenges, a nature research question comes:

075 *(Q) How to leverage the personalized knowledge captured in the first fine-tuned model to*
 076 *update any evolving LLMs?*

077 To address this question, we introduce PORTLLM, training-free framework that enables seamless
 078 transfer of domain-specific knowledge across evolving models. PORTLLM leverages model patches
 079 derived from LoRA, allowing users to port fine-tuned knowledge from one model iteration to an-
 080 other while preserving or even enhancing the performance of a downstream task. We show that
 081 our model patches are portable across model updates. If the downstream user fine-tunes a version
 082 of the model that has long become obsolete, they can simply add the model patches to the newer
 083 model, maintaining or boosting their performance on the downstream task. PORTLLM eliminates
 084 the need for costly periodic fine-tuning, offering a scalable solution for maintaining task-specific
 085 performance across different model versions. Our contributions can be summarized as follows:

- 087 ❶ We introduce PORTLLM, a training-free framework designed to transfer knowledge between
 088 different versions of an evolving LLM. Given two model versions, PORTLLM leverages task-
 089 specific model patches extracted from a pretrained LLM and seamlessly applies them to the
 090 updated version of the pretrained LLM. This process allows the updated model to achieve com-
 091 parable, and in some cases improved, performance on downstream tasks — without any need for
 092 fine-tuning.
- 093 ❷ *Why do our model patches work?* We address this question through both theoretical analysis
 094 and empirical investigation. Our findings reveal that certain terms in the model patch are effec-
 095 tively negligible, enabling us to create a simplified version of the patch that requires no train-
 096 ing. Consequently, adding the simplified model patches alone is sufficient to achieve improved
 097 performance on the downstream task. Furthermore, we examine the impact of the pretraining
 098 dataset on downstream tasks, demonstrating that our framework can harness the benefits of con-
 099 tinued pretraining across different model updates, across different pretraining datasets including
 100 {OpenOrca, SlimOrca, OpenPlatypus, AlpacaGPT4}.
- 101 ❸ We conduct extensive experiments across a series of **seven** downstream tasks, including
 102 Question-Answering Tasks {BoolQ, SST-2} (Wang, 2018; Wang et al., 2019), Similarity and
 103 Paraphrase Tasks {MRPC} (Wang, 2018), Inference Tasks {RTE, WNLI} (Wang, 2018), and
 104 Reasoning Tasks {WinoGrande, GSM8K} (Sakaguchi et al., 2021; Cobbe et al., 2021). To further
 105 demonstrate the robustness and broad applicability of our approach, we evaluate it on multiple
 106 model architectures, such as Mistral-7B, Llama2-7B, Llama3.1-8B, and Gemma2-9B.
 107 Additionally, we explore the applicability of our method on full-weight continued pretraining
 compared to LoRA-based continued pretraining and show the effectiveness of our method by

quantifying the gains on GPU memory usage (of up to $12.2\times$ reduction), GPU hours, and decrease in the number of trainable parameters (to zero trainable parameters).

2 RELATED WORKS

Large Language Models (LLMs). LLMs have transformed natural language processing, enabling models to perform complex tasks with remarkable accuracy and generalization. Models like GPT-3 (Brown et al., 2020), BERT (Devlin et al., 2019), and T5 (Raffel et al., 2023) have set benchmarks across a range of NLP tasks, from translation and summarization to question answering and text generation (Vaswani et al., 2023; Zhang et al., 2020; Rajpurkar et al., 2016). More recently, models like Llama (Touvron et al., 2023; Dubey et al., 2024), Mistral (Jiang et al., 2023), and Gemma (Team et al., 2024) have pushed the boundaries further by optimizing both performance and computational efficiency. [LLama, Mistral, and Gemma represent recent advances in LLM architectures, each offering improvements in efficiency and performance.](#) However, even with such improvements, the performance on domain-specific downstream tasks is sub-par making fine-tuning necessary. [In this paper, we propose a training-free solution that enables the seamless transfer of personalized knowledge across evolving LLMs, reducing the need for costly fine-tuning and enhancing accessibility.](#)

Parameter Efficient Fine-tuning (PEFT). The rapid growth in the size of pretrained LLMs has posed significant challenges for efficiently fine-tuning LLMs to specific downstream tasks. To address this, numerous PEFT methods have been developed, aiming to balance efficiency and accuracy. Early approaches focused on inserting trainable adapters—feed-forward networks placed between the layers of the pretrained model (Houlsby et al., 2019; Lin et al., 2020). Recent advancements have led to more sophisticated adapter-based PEFT methods (Mahabadi et al., 2021; Pfeiffer et al., 2020; Luo et al., 2023) [including LMaaS \(Sun et al., 2022\) for service-oriented adaptation and kNN-Adapter \(Huang et al., 2023\) for retrieval-augmented fine-tuning.](#) A notable example is LoRA (Hu et al., 2021), which introduces trainable low-rank weight perturbations to the pretrained model, significantly reducing the number of parameters required for fine-tuning. LoRA’s key innovation lies in its use of the product of two low-rank matrices to approximate weight changes. Building upon this concept, [several methods have emerged including Q-LoRA \(Dettmers et al., 2023\), ComBLM \(Ormazabal et al., 2023\), and IPA \(Lu et al., 2023\).](#) Concurrently, prompt-based learning methods have demonstrated effectiveness across various NLP tasks. Methods such as prompt-tuning (Lester et al., 2021), prefix-tuning (Li & Liang, 2021) [and more recent approaches like Proxy-Tuning \(Liu et al., 2024\) and BBox-Adapter \(Sun et al., 2024\)](#) incorporate learnable continuous embeddings into the model’s hidden states. They condition the frozen model to adapt to specific tasks without modifying the underlying architecture. Despite these advances, fine-tuning each updated LLM with PEFT to equip personalized knowledge remains highly costly, and how PEFT can bridge the gap in personalized settings within this evolving environment in a portable manner is yet to be fully explored. To this end, we develop in this paper the theory behind portable model patches that can be plugged into an updated model to carry over the personalized knowledge from the first fine-tuned model.

3 METHODOLOGY

3.1 PRELIMINARIES

Transformers. Transformer models (Vaswani et al., 2023) is an architecture that has revolutionized NLP and other sequence-based tasks. It consists of two key components: (1) Multi-Head Self-Attention and (2) Feed-Forward Neural Network. The Multi-Head Self-Attention mechanism is the core innovation of transformers. It computes the weighted representation of the input sequence where each token attends to every other token. Suppose we are given an input $X \in \mathbb{R}^{n \times d}$ where n refers to the sequence length and d is the hidden dimension of the transformer model. Then for any given attention head i with a total of H heads, we define the following three matrices: query matrix $W_{q_i} \in \mathbb{R}^{d \times d_H}$, key matrix $W_{k_i} \in \mathbb{R}^{d \times d_H}$ and value matrix $W_{v_i} \in \mathbb{R}^{d \times d_H}$, where $d_H = d/H$. Given these, we can compute the self-attention for the i th head as follows

$$h_i = \text{Softmax} \left(\frac{XW_{q_i}(XW_{k_i})^T}{\sqrt{d_H}} XW_{v_i} \right), \quad i = 1, \dots, H. \quad (1)$$

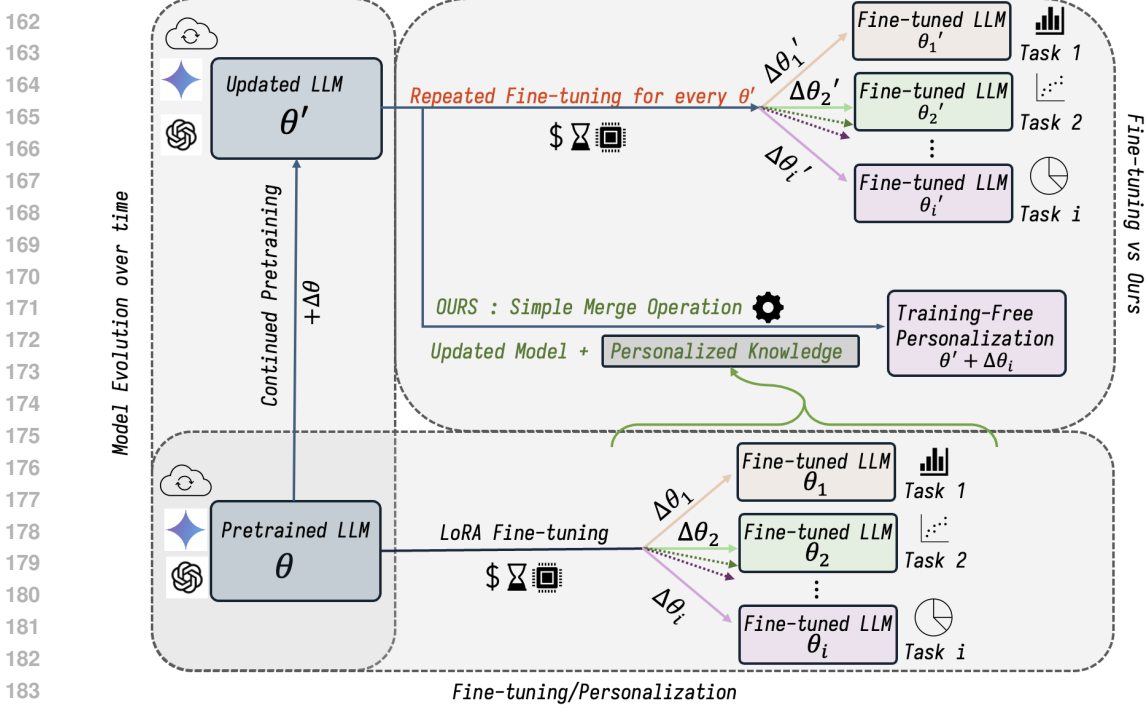


Figure 1: The diagram illustrates the core components of PORTLLM, a training-free framework to port personalized knowledge between evolving LLMs. Initially, a pretrained LLM is fine-tuned using LoRA. We transfer this task-specific knowledge without requiring the newer updated model to be fine-tuned again. This allows for continual performance improvements on downstream tasks without additional periodic fine-tuning.

The outputs of the H attention heads are then concatenated as follows:

$$\text{Multi-head Self-Attention}(X) = \text{Concatenate}(h_1, h_2, \dots, h_H)W_o, \quad (2)$$

where $W_o \in \mathbb{R}^{d \times d}$ is a projection matrix that combines the outputs of the different heads back into the model’s hidden dimension d . After the Multi-head Self-Attention, the output is passed through a position-wise feed-forward network that consists of two linear transformations and a nonlinear activation function (like ReLU or GELU). Given the weight matrix of the first linear layer $W_{\text{up}} \in \mathbb{R}^{d \times d_m}$, the weight matrix of the second layer $W_{\text{down}} \in \mathbb{R}^{d_m \times d}$, bias terms $b_1 \in \mathbb{R}^{d_m}$, $b_2 \in \mathbb{R}^d$, and a non-linear activation function $\sigma(\cdot)$ where d_m is the hidden dimension, Feed-Forward Network is applied independently to each position in the sequence as follows

$$\text{Feed-Forward Network}(X) = \sigma(XW_{\text{up}} + b_1)W_{\text{down}} + b_2. \quad (3)$$

Furthermore, these two layers are wrapped with residual connections and layer normalization.

Low-Rank Adaptation (LoRA). Consider a transformer model where $W_0 \in \mathbb{R}^{d \times d}$ is the pre-trained weight matrix, which could be a weight matrix for any layer in the transformer. In a typical fine-tuning setup, the weights W_0 are updated during training to adapt the model to a specific task. This update requires storing and computing the entire matrix W_0 during training, which becomes computationally expensive for large models. Instead of updating the full weight matrix W_0 , LoRA (Hu et al., 2021) assumes that the weight update $\Delta W \in \mathbb{R}^{d \times d}$, essentially the difference between pretrained weights W_0 and the hypothetical fine-tuned weight, can be approximated by a low-rank decomposition:

$$\Delta W = BA, \quad (4)$$

where $B \in \mathbb{R}^{d \times r}$ and $A \in \mathbb{R}^{r \times d}$ are trainable matrices, while r is the rank of the decomposition with $r \ll d$. In this setup, the full weight update matrix ΔW is replaced by the product of two smaller matrices, B and A , drastically reducing the number of trainable parameters from d^2 to $2rd$. Hence, the fine-tuned model weights we can be trained as follows:

$$W_{\text{new}} = W_0 + \Delta W = W_0 + BA. \quad (5)$$

By doing this, LoRA reduces the number of parameters that need to be trained while still allowing the model to adapt to new tasks.

3.2 PROPOSED TRAINING-FREE FRAMEWORK: PORTLLM

Notations and Assumptions. We refer to the pretrained LLM as the first version of the model, denoted by θ , and the updated continued pretrained model as θ' , as illustrated in Figure 2. We also assume that to get to θ' , the provider does continued pretraining using LoRA, where $\Delta\theta$ denotes this adapter, however empirical experiments in Section 4.4 show that even if the provider does full weight continued pretraining on the newer dataset, our method still holds. We denote this full weight updated model as ϕ . Similarly, for any downstream user i , we have a corresponding dataset denoted d_i . The base model fine-tuned on this dataset d_i is denoted by θ_i . We can also rewrite θ_i in terms of its LoRA update as $\theta_i = \theta + \Delta\theta_i$. Consequently, if we fine-tune updated model θ' for i th downstream task, we have $\theta'_i = \theta' + \Delta\theta'_i$. We further assume that a personalization adaptor $\Delta\theta_i$ or $\Delta\theta'_i$ has a rank that is much smaller than that of a continued pretrained adaptor $\Delta\theta$ or $\Delta\theta'$.

Proposed Method of PORTLLM. PORTLLM aims to approximate the fine-tuned updated model θ'_i by applying the older personalization adaptor/model patch $\Delta\theta_i$ to the continued pretrained model θ' . It will be shown in Section 3.3 that the older model patch $\Delta\theta_i$ may be used in lieu of the newer model patch $\Delta\theta'_i$, namely,

$$\theta'_i = \theta' + \Delta\theta'_i \approx \theta' + \Delta\theta_i. \quad (6)$$

In other words, one can readily add the extra knowledge $\Delta\theta_i$ from the previous fine-tuning process to the newest LLM θ' . Throughout our experimental section, we perform experiments with this approximated patching process.

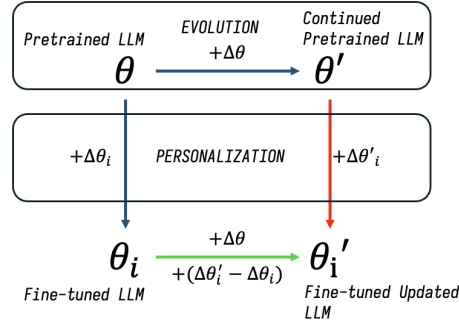


Figure 2: LLM’s evolution & personalization cycle.

3.3 ANALYSIS OF OUR PROPOSED PORTABILITY

Theoretical Justification. The fine-tuned updated model θ'_i can be decomposed into a naive update term and a residual matrix R as follows:

$$\theta'_i = \theta' + \Delta\theta'_i \quad (7a)$$

$$= \underbrace{(\theta' + \Delta\theta_i)}_{\text{Naive Update } \hat{\theta}'_i} + \underbrace{(\Delta\theta'_i - \Delta\theta_i)}_{\text{Residual Matrix } R}. \quad (7b)$$

Lemma 1 (informal): We claim that the residual matrix R is negligible compared to the naive update $\hat{\theta}'_i$. The key reason is that the model patches $\Delta\theta'_i$ and $\Delta\theta_i$ are both low rank (recall the assumption in Section 3.2), whereas the pretrained models θ and θ' are primarily full rank matrices. We provide a formal proof in Appendix C.

Empirical Validation. We empirically show that the difference between two personalization updates, $R = \Delta\theta'_i - \Delta\theta_i$, is negligible when compared to naive update term, $\theta' + \Delta\theta_i$. We use Frobenius norm, $\|\cdot\|_F$, and the maximum singular value, σ_{\max} , to measure the magnitudes of matrices. The results are summarized in Table 1 across four different downstream tasks {BoolQ, MRPC, RTE, WNLI}. We can see that the σ_{\max} for first term are on average 66× and the $\|\cdot\|_F$ is 136× bigger in the favor of the first term, which implies that R is comparatively negligible, hence our model patch can be simplified as shown in (6).

Table 1: Comparison of the terms making up our framework across different datasets.

Term		BoolQ	MRPC	RTE	WNLI
$\theta' + \Delta\theta_i$	σ_{\max}	7.37	7.37	7.37	7.37
	$\ \cdot\ _F$	16.80	16.80	16.81	16.81
$\Delta\theta'_i - \Delta\theta_i$	σ_{\max}	0.19	0.14	0.10	0.08
	$\ \cdot\ _F$	0.21	0.13	0.12	0.09
$\sigma_{\max}/\sigma_{\max}$		38.77	51.37	76.32	96.24
$\ \cdot\ _F/\ \cdot\ _F$		79.04	126.70	145.43	194.30

Table 2: Zero-shot performance comparison of model patches and baselines models on Mistral-7B, using the *OpenOrca* dataset for continued pretraining.

Model Version	BoolQ Accuracy	SST-2 Accuracy	MRPC Accuracy/F1	RTE Accuracy	WinoGrande Accuracy	WNLI Accuracy	GSM8K Accuracy
Pretrained LLM θ	83.58	66.86	65.20 / 73.70	67.51	74.11	57.76	6.37
Updated LLM θ'	87.46	82.91	74.75 / 83.73	75.09	75.06	57.72	15.16
Fine-tuned LLM θ_i	91.01	95.99	89.46 / 92.62	87.73	85.95	83.11	34.04
Fine-tuned Updated LLM θ'_i	90.67	96.22	89.20 / 93.03	89.89	86.05	82.08	34.95
$\theta' + \Delta\theta_i$ (Ours)	90.24	96.10	88.73 / 92.10	89.17	85.01	83.10	41.32

4 EXPERIMENTS

Datasets and Architecture. We evaluate our framework on a diverse set of datasets to demonstrate PORTLLM universality and effectiveness across various downstream tasks and domains. Specifically, we leverage datasets from the *GLUE* (Wang, 2018), *SuperGLUE* (Wang et al., 2019), *WinoGrande* (Sakaguchi et al., 2021) and *GSM8K* (Cobbe et al., 2021) benchmarks commonly used for such evaluation in literature. For Question Answering tasks, we utilize *BoolQ* (from *SuperGLUE*) and *SST-2* (from *GLUE*); for Similarity and Paraphrase Tasks, the *MRPC* (from *GLUE*) dataset; for Inference Tasks, the *RTE* and *WNLI* (both from *GLUE*) datasets; and lastly for Reasoning Tasks, we employ *WinoGrande* and *GSM8K*. This broad spectrum of tasks enables a comprehensive evaluation of our model’s performance across diverse downstream applications. For continued pretraining datasets, we use the following: *OpenOrca* (Lian et al., 2023a), *SlimOrca* (Lian et al., 2023b), *OpenPlatypus* (Lee et al., 2023) and *AlpacaGPT4* (Peng et al., 2023). Additionally, we conduct extensive experiments across multiple model architectures to demonstrate the generalizability of our framework. Specifically, we test our method on Mistral-7B (Jiang et al., 2023), Llama2-7B (Touvron et al., 2023), Llama3.1-8B (Dubey et al., 2024), and Gemma2-9B (Team et al., 2024), showcasing the robustness and adaptability of our approach across different LLMs.

Training Details. To simulate the progression of time, we employ continued pretraining, where we transition from θ to θ' by taking a pretrained model and further pretraining it on a specific dataset using LoRA (Hu et al., 2021). In all continued pretraining scenarios, we maintain a constant rank $r = 64$ and $\alpha = 128$ with a learning rate of 0.0001 and 4 epochs. For downstream tasks, we also use LoRA, but in this case, we set the rank $r = 8$ consistently to ensure a fair comparison across tasks. Furthermore, for all LoRA applications we optimize all the attention layers (Key, Value, Query, Projection), and all Feed Forward Network layers (Up Projection, Down Projection and Gate Projection, where applicable). For each downstream fine-tuning, we use a constant learning rate of 0.0004 while the number of epochs for each dataset $\{\textit{BoolQ}, \textit{SST-2}, \textit{MRPC}, \textit{RTE}, \textit{WinoGrande}, \textit{WNLI}, \textit{GSM8K}\}$ is as follows $\{5, 5, 5, 5, 3, 5, 1\}$. Lastly, for fine-tuning on specific downstream dataset mentioned, we solely use the train split, and evaluate on test split.

Evaluation Metrics. We use the *Language Model Evaluation Harness* (Gao et al., 2024a) by EleutherAI to assess the performance of all trained and fine-tuned models across the datasets in our experiments. All evaluations are conducted in a *zero-shot* setting rather than a few-shot setting. For datasets $\{\textit{BoolQ}, \textit{SST-2}, \textit{RTE}, \textit{WinoGrande}, \textit{WNLI}\}$, we employ accuracy as the primary evaluation metric. In the case of $\{\textit{MRPC}\}$, we utilize both accuracy and F1 score to provide a more comprehensive evaluation. For $\{\textit{GSM8K}\}$, we had two evaluation options: (1) Flexible Match Accuracy or (2) Exact Match Accuracy. Due to poor zero-shot performance of the models on *GSM8K* for exact matches, we opted for Flexible Match Accuracy.

4.1 SUPERIORITY OF PORTLLM FRAMEWORK

In this section, we compare the performance of our model patches against several baseline models, including the pretrained LLM θ , the updated model using continued pretraining θ' , the fine-tuned model θ_i , and the updated fine-tuned model θ'_i . For consistency, all models are variations of Mistral-7B, while continued pretraining dataset is *OpenOrca*. Importantly, the performance is evaluated under zero-shot setting across all the datasets. The results are summarized in Table 2.

Table 3: Performance comparison of model patches $\Delta\theta_i$ across four downstream tasks $\{BoolQ, MRPC, WNLI, WinoGrande\}$ using different continued pretraining datasets $\{OpenOrca, SlimOrca, OpenPlatypus, AlpacaGPT4\}$. All models are based on `Mistral-7B`.

Dataset	Model	BoolQ Accuracy	MRPC Accuracy	WNLI Accuracy	WinoGrande Accuracy
OpenOrca	Updated Model θ'	87.46	74.75	57.72	75.06
	Ours $\theta' + \Delta\theta_i$	90.24 ($\uparrow 2.78$)	88.73 ($\uparrow 13.98$)	83.10 ($\uparrow 25.38$)	85.01 ($\uparrow 9.95$)
SlimOrca	Updated Model θ'	87.16	74.76	64.79	74.98
	Ours $\theta' + \Delta\theta_i$	90.07 ($\uparrow 2.91$)	87.75 ($\uparrow 12.99$)	83.09 ($\uparrow 18.30$)	85.59 ($\uparrow 10.61$)
OpenPlatypus	Updated Model θ'	83.73	70.10	53.52	73.95
	Ours $\theta' + \Delta\theta_i$	90.34 ($\uparrow 6.61$)	90.20 ($\uparrow 20.10$)	80.28 ($\uparrow 26.76$)	83.58 ($\uparrow 9.63$)
AlpacaGPT4	Updated Model θ'	83.94	71.32	56.34	74.82
	Ours $\theta' + \Delta\theta_i$	90.52 ($\uparrow 6.58$)	89.22 ($\uparrow 17.90$)	84.51 ($\uparrow 28.17$)	84.93 ($\uparrow 10.11$)

① Compared to the zero-shot accuracy of updated model θ' , applying our model patches can result in a significant performance gains, with improvements up to $2.7\times$. Notably, no additional training is required when applying these patches, as the process simply involves a merge operation. Across all evaluated datasets $\{BoolQ, SST-2, MRPC, RTE, WinoGrande, WNLI, GSM8K\}$, we observe substantial zero-shot performance gains of $\{2.7\%, 13.19\%, 13.98\%, 14.08\%, 9.95\%, 25.38\%, 26.16\%\}$, respectively. This implies that our model patches are capable of transferring personalized knowledge across the different model versions.

② Comparing the performance of our model patches applied to the updated model $\theta' + \Delta\theta_i$ with that of the fine-tuned model θ_i , we observe that our method successfully transfers most of the downstream task-specific knowledge, yielding comparable results. As shown in Table 2, for tasks $\{BoolQ, MRPC, WinoGrande, WNLI\}$, the performance is nearly identical, with a maximum difference of only 0.77% in favor of the fine-tuned model. However, in tasks like $\{SST-2, RTE, GSM8K\}$, our approach outperforms the fine-tuned model by $\{0.11\%, 1.44\%, 7.28\%\}$, respectively. These results suggest that, when paired with a pretraining dataset that enhances performance for a specific task, our model patches can further leverage this advantage to improve downstream task performance in certain cases.

③ Moreover, our method performs on par with the fine-tuned updated model ($\theta' + \Delta\theta_i$ compared to θ'_i), as evident from the comparison of the last two rows in Table 2. The difference between the two approaches are minimal when it comes to performance, with a maximum variation of just 1.04% observed in the case of *WinoGrande*. Notably, while one method requires fine-tuning, our approach remains completely training-free. Additionally, for certain downstream tasks such as *WNLI* and *GSM8K*, our method outperforms the fine-tuned updated model by 1.02% and 6.37%, respectively. This demonstrates that our approach not only provides comparable results but can, in some instances, surpass the performance of a fine-tuned evolved model.

4.2 CONSISTENT RESULTS ACROSS DIFFERENT PRETRAINING DATASETS

In this section, we investigate the impact of different pretraining datasets on our model patches $\Delta\theta_i$ and assess whether our method can effectively leverage updates obtained through continued pretraining. We conduct a comparative analysis across four downstream datasets – $\{BoolQ, MRPC, WNLI, WinoGrande\}$ – alongside four distinct continued pretraining datasets: *OpenOrca*, *SlimOrca*, *OpenPlatypus*, and *AlpacaGPT4*. Consistent with our previous section, all experiments utilize the `Mistral-7B` model. The results of this analysis are summarized in Table 3.

① The results presented in Table 3 demonstrate that our model patches exhibit strong portability across different downstream tasks, irrespective of the continued pretraining dataset used. For each specific downstream task, we observe substantial improvements in zero-shot performance compared to the updated model θ' across all pretraining datasets. For instance, in the case of *WNLI*, the performance boosts are $\{25.38\%, 18.30\%, 26.76\%, 28.17\%\}$ for $\{OpenOrca, SlimOrca, OpenPlatypus, AlpacaGPT4\}$ datasets, respectively. A similar trend of significant improvement is also evident across other downstream tasks.

Table 4: Performance analysis of model patches across various architectures $\{\text{Mistral-7B}, \text{Llama2-7B}, \text{Llama3.1-8B}, \text{Gemma2-9B}\}$ on four downstream tasks $\{\text{BoolQ}, \text{MRPC}, \text{WNLI}, \text{WinoGrande}\}$ under four different model settings. For each downstream task **Orange** highlights the best performance for each model architecture.

Model	Version	BoolQ Accuracy	MRPC Accuracy/F1	WNLI Accuracy	WinoGrande Accuracy
Mistral 7B	Pretrained Model θ	83.58	65.20 / 73.70	57.76	74.11
	Updated Model θ'	87.46	74.75 / 83.73	57.72	75.06
	Fine-tuned Model θ_i	91.01	89.46 / 92.62	83.11	85.95
	Ours $\theta' + \Delta\theta_i$	90.24	88.73 / 92.10	83.10	85.01
Llama 2 7B	Pretrained Model θ	77.74	69.12 / 81.52	45.07	69.06
	Updated Model θ'	82.69	69.61 / 81.60	47.89	70.48
	Fine-tuned Model θ_i	88.21	88.97 / 92.01	57.75	75.45
	Ours $\theta' + \Delta\theta_i$	88.32	89.95 / 92.56	53.77	76.87
Llama 3.1 8B	Pretrained Model θ	82.35	66.91 / 77.54	59.15	73.56
	Updated Model θ'	85.63	75.00 / 83.60	61.95	73.64
	Fine-tuned Model θ_i	90.22	84.31 / 89.51	83.10	85.71
	Ours $\theta' + \Delta\theta_i$	90.03	89.71 / 92.71	81.69	84.85
Gemma 2 9B	Pretrained Model θ	83.98	68.63 / 74.19	57.75	74.19
	Updated Model θ'	88.41	77.21 / 84.93	74.65	76.72
	Fine-tuned Model θ_i	91.38	91.42 / 93.83	83.20	83.98
	Ours $\theta' + \Delta\theta_i$	91.16	90.69 / 93.17	88.73	83.82

⊗ We further observe from Table 3 that certain pretraining datasets can either enhance or detract from the zero-shot performance of θ' on specific downstream tasks, and this effect carries over to our frameworks to some degree. For instance, continued pretraining on *OpenPlatypus* leads to a decrease in performance on the *WNLI* dataset. Consequently, the addition of our model patch in this scenario results in the lowest accuracy for this particular downstream task among all the pretraining datasets evaluated.

4.3 CONSISTENT RESULTS ACROSS DIFFERENT MODEL ARCHITECTURES

This section provides a comprehensive analysis of our model patches across various architectures to evaluate their performance. We examine four different model architectures: $\{\text{Mistral-7B}, \text{Llama2-7B}, \text{Llama3.1-8B}, \text{Gemma2-9B}\}$, assessing their effectiveness on four distinct downstream tasks $\{\text{BoolQ}, \text{MRPC}, \text{WNLI}, \text{WinoGrande}\}$. Performance is evaluated under four settings : (1) pretrained model, (2) continued pretrained model or Updated Model, (3) fine-tuned model, and (4) our model patches ported to the updated model. The *OpenOrca* dataset is used for our continued pretraining in this analysis. The results are summarized in Table 4

⊙ The results across different model architectures indicate that our training-free model patches significantly enhance zero-shot performance for all downstream tasks. In each case, our approach matches personalized performance (fine-tuned model), and in certain instances, it even surpasses it. For example, with *Gemma2-9B*, when the personalized performance exceeds our method, the difference in accuracy is at most 0.73%, which can be considered negligible. Conversely, in scenarios where our method outperforms personalized performance, we observe improvements of up to 5.53%. A similar trend is noted across the other model architectures, as detailed in Table 4.

⊗ Additionally, we observe that fine-tuning is essential for achieving optimal zero-shot performance on downstream tasks. Across all model architectures, the zero-shot performance of both the pretrained model θ and the updated model θ' is subpar, with particularly poor results noted on tasks like *WNLI*. This reinforces the notion that excellent performance necessitates some form of fine-tuning, further motivating the need for our training-free framework. Another significant finding is the slight performance improvement for downstream tasks across all model architectures due to continued

Table 5: Evaluation of model patches added to `Mistral-7B` with full weight continued pretraining on the OpenOrca dataset across various downstream tasks.

Model Version	BoolQ Accuracy	SST-2 Accuracy	MRPC Accuracy/F1	RTE Accuracy	WinoGrande Accuracy	WNLI Accuracy	GSM8K Accuracy
Full Weight Updated Model ϕ	86.61	93.81	77.21 / 85.31	75.09	72.77	63.38	20.55
$\phi + \Delta\theta_i$ (Ours)	89.88	95.53	87.25 / 90.97	90.61	85.08	80.28	41.24

pretraining. Therefore, it is advisable for the downstream user to utilize the updated model weights, as this may provide beneficial enhancements in performance.

4.4 PORTLLM ALSO WORKS WITH FULL WEIGHT CONTINUED PRETRAINING

For our theoretical analysis, we initially assumed that continued pretraining was conducted using LoRA. However, we aim to investigate whether our method is effective across model evolution when the updates occur through full weight continued pretraining. Such a model is denoted ϕ . To evaluate this, we utilize `Mistral-7B`, which has undergone full weight continued pretraining on the OpenOrca dataset, and incorporate our model patches for various downstream tasks. We then compare the performance of these patched models against the zero-shot performance of ϕ to assess the improvements attributable to our model patches. The results across various downstream tasks are summarized in Table 5.

We find that our model patches can be effectively applied to a continued pretrained model utilizing full weight updates, rather than relying solely on LoRA. Across all evaluated datasets – $\{BoolQ, SST-2, MRPC, RTE, WinoGrande, WNLI, GSM8K\}$ – we observe significant performance improvements of $\{3.27\%, 1.72\%, 10.04\%, 15.52\%, 12.31\%, 16.90\%, 20.69\%\}$, respectively, compared to the zero-shot performance of the Updated Model.

4.5 COMPUTING EFFICIENCY COMPARISON OF PORTLLM

This section evaluates the performance of our method from an efficiency perspective. We employ the following metrics for comparison: (1) Number of Trainable Parameters, (2) GPU Memory Utilization, and

(3) GPU Hours. We analyze the merging of our model patches in relation to model fine-tuning using LoRA to achieve comparable performance. For LoRA fine-tuning calculations, we have the following settings: Downstream task `SST-2` for `Mistral-7B`, with local Batch Size of 4 and 5 Epochs. The results are summarized in Table 6.

Compared to downstream fine-tuning using LoRA, our methods offers plug-and-play solution with no trainable parameters, resulting in a reduction of nearly 20 million parameters that need to be trained. This training-free paradigm not only conserves resources but also saves up to $12.2\times$ GPU Memory, reducing the requirement from 350 GB for LoRA to just 28.7 GB during the merge operation of model patches. Additionally, the merge operation can be executed in mere seconds, in start contrast to the hours required for fine-tuning. This opens many other doors for applications of our model patches. PORTLLM demonstrates the potential for on-device, training-free models for various down-stream tasks without the need for fine-tuning. Furthermore, it reduces the need for expensive cloud infrastructure, especially in large-scale fine-tuning.

5 CONCLUSION

In this paper, we propose PORTLLM, a framework aimed at addressing the challenges faced by downstream users of pretrained LLMs when adapting to frequent model evolutions over time. By leveraging lightweight model patches, PORTLLM offers a training-free, cost-effective solution to

seamlessly transfer domain-specific knowledge between different iterations of LLMs. This enables users to maintain, and sometimes even enhance, their models’ performance on specialized tasks without the need for repeated fine-tuning or extensive computational resources. Through extensive empirical evaluations across a set of tasks and models, we demonstrate that our method not only preserves performance but can also leverage the continual updates in pretraining LLMs, offering substantial gains in-task specific performance. Moreover, we provide theoretical insights into the portability of these model patches, highlighting the underlying factors that make them effective across evolving model versions. Looking forward, PORTLLM paves the way for more robust and adaptable solutions in the evolving landscape of LLM personalization, offering another avenue for training-free adaptation. Furthermore, future endeavours will aim at developing such methods that work across different model architecture, including using techniques from model merging.

6 REPRODUCIBILITY STATEMENT

To ensure reproducibility, we provide detailed descriptions of datasets, model architectures, training settings, and evaluation metrics used in our experiments in Section 4. The same section also dives deep into the hyper-parameters used for all the tasks mentioned in our paper, including LoRA fine-tuning and downstream evaluation. Furthermore, we have also provided all the training scripts alongside the hyper-parameters as supplementary material so that results from our papers can be reproduced with minimal effort. Lastly, the datasets and model architectures utilized in this paper are open-source and publicly available for anyone’s use. Each dataset, as well as model, have been cited accordingly so that anyone can reproduce the experiments.

REFERENCES

- Josh Achiam, Steven Adler, Sandhini Agarwal, Lama Ahmad, Ilge Akkaya, Florencia Leoni Aleman, Diogo Almeida, Janko Altenschmidt, Sam Altman, Shyamal Anadkat, et al. Gpt-4 technical report. *arXiv preprint arXiv:2303.08774*, 2023.
- Antonis Antoniadou, Xinyi Wang, Yanai Elazar, Alfonso Amayuelas, Alon Albalak, Kexun Zhang, and William Yang Wang. Generalization vs memorization: Tracing language models’ capabilities back to pretraining data. *arXiv preprint arXiv:2407.14985*, 2024.
- Rishi Bommasani, Drew A. Hudson, Ehsan Adeli, Russ Altman, Simran Arora, Sydney von Arx, Michael S. Bernstein, Jeannette Bohg, Antoine Bosselut, Emma Brunskill, Erik Brynjolfsson, S. Buch, Dallas Card, Rodrigo Castellon, Niladri S. Chatterji, Annie S. Chen, Kathleen A. Creel, Jared Davis, Dora Demszky, Chris Donahue, Moussa Doumbouya, Esin Durmus, Stefano Ermon, John Etchemendy, Kawin Ethayarajh, Li Fei-Fei, Chelsea Finn, Trevor Gale, Lauren E. Gillespie, Karan Goel, Noah D. Goodman, Shelby Grossman, Neel Guha, Tatsunori Hashimoto, Peter Henderson, John Hewitt, Daniel E. Ho, Jenny Hong, Kyle Hsu, Jing Huang, Thomas F. Icard, Saahil Jain, Dan Jurafsky, Pratyusha Kalluri, Siddharth Karamcheti, Geoff Keeling, Fereshte Khani, O. Khattab, Pang Wei Koh, Mark S. Krass, Ranjay Krishna, Rohith Kuditipudi, Ananya Kumar, Faisal Ladhak, Mina Lee, Tony Lee, Jure Leskovec, Isabelle Levent, Xiang Lisa Li, Xuechen Li, Tengyu Ma, Ali Malik, Christopher D. Manning, Suvir P. Mirchandani, Eric Mitchell, Zanele Muniyikwa, Suraj Nair, Avani Narayan, Deepak Narayanan, Benjamin Newman, Allen Nie, Juan Carlos Niebles, Hamed Nilforoshan, J. F. Nyarko, Giray Ogut, Laurel Orr, Isabel Papadimitriou, Joon Sung Park, Chris Piech, Eva Portelance, Christopher Potts, Aditi Raghunathan, Robert Reich, Hongyu Ren, Frieda Rong, Yusuf H. Roohani, Camilo Ruiz, Jack Ryan, Christopher R’e, Dorsa Sadigh, Shiori Sagawa, Keshav Santhanam, Andy Shih, Krishna Parasuram Srinivasan, Alex Tamkin, Rohan Taori, Armin W. Thomas, Florian Tramèr, Rose E. Wang, William Wang, Bohan Wu, Jiajun Wu, Yuhuai Wu, Sang Michael Xie, Michihiro Yasunaga, Jiaxuan You, Matei A. Zaharia, Michael Zhang, Tianyi Zhang, Xikun Zhang, Yuhui Zhang, Lucia Zheng, Kaitlyn Zhou, and Percy Liang. On the opportunities and risks of foundation models. *ArXiv*, 2021. URL <https://crfm.stanford.edu/assets/report.pdf>.
- Tom B. Brown, Benjamin Mann, Nick Ryder, Melanie Subbiah, Jared Kaplan, Prafulla Dhariwal, Arvind Neelakantan, Pranav Shyam, Girish Sastry, Amanda Askell, Sandhini Agarwal, Ariel Herbert-Voss, Gretchen Krueger, Tom Henighan, Rewon Child, Aditya Ramesh, Daniel M. Ziegler, Jeffrey Wu, Clemens Winter, Christopher Hesse, Mark Chen, Eric Sigler, Mateusz

- 540 Litwin, Scott Gray, Benjamin Chess, Jack Clark, Christopher Berner, Sam McCandlish, Alec
541 Radford, Ilya Sutskever, and Dario Amodei. Language models are few-shot learners, 2020. URL
542 <https://arxiv.org/abs/2005.14165>.
- 543
- 544 Nuo Chen, Yuhan Li, Jianheng Tang, and Jia Li. Graphwiz: An instruction-following language
545 model for graph problems. *arXiv preprint arXiv:2402.16029*, 2024.
- 546 Karl Cobbe, Vineet Kosaraju, Mohammad Bavarian, Mark Chen, Heewoo Jun, Lukasz Kaiser,
547 Matthias Plappert, Jerry Tworek, Jacob Hilton, Reiichiro Nakano, Christopher Hesse, and John
548 Schulman. Training verifiers to solve math word problems. *arXiv preprint arXiv:2110.14168*,
549 2021.
- 550 Tim Dettmers, Artidoro Pagnoni, Ari Holtzman, and Luke Zettlemoyer. Qlora: Efficient finetuning
551 of quantized llms, 2023. URL <https://arxiv.org/abs/2305.14314>.
- 552
- 553 Jacob Devlin, Ming-Wei Chang, Kenton Lee, and Kristina Toutanova. Bert: Pre-training of deep
554 bidirectional transformers for language understanding, 2019. URL <https://arxiv.org/abs/1810.04805>.
- 555
- 556 Abhimanyu Dubey, Abhinav Jauhri, Abhinav Pandey, Abhishek Kadian, Ahmad Al-Dahle, Aiesha
557 Letman, Akhil Mathur, Alan Schelten, Amy Yang, Angela Fan, et al. The llama 3 herd of models.
558 *arXiv preprint arXiv:2407.21783*, 2024.
- 559
- 560 Leo Gao, Jonathan Tow, Baber Abbasi, Stella Biderman, Sid Black, Anthony DiPofi, Charles Foster,
561 Laurence Golding, Jeffrey Hsu, Alain Le Noac’h, Haonan Li, Kyle McDonell, Niklas Muen-
562 nighoff, Chris Ociepa, Jason Phang, Laria Reynolds, Hailey Schoelkopf, Aviya Skowron, Lintang
563 Sutawika, Eric Tang, Anish Thite, Ben Wang, Kevin Wang, and Andy Zou. A framework for
564 few-shot language model evaluation, 07 2024a. URL <https://zenodo.org/records/12608602>.
- 565
- 566 Ziqi Gao, Xiangguo Sun, Zijing Liu, Yu Li, Hong Cheng, and Jia Li. Protein multimer structure
567 prediction via prompt learning. *arXiv preprint arXiv:2402.18813*, 2024b.
- 568
- 569 Neil Houlsby, Andrei Giurgiu, Stanislaw Jastrzebski, Bruna Morrone, Quentin de Laroussilhe, An-
570 drea Gesmundo, Mona Attariyan, and Sylvain Gelly. Parameter-efficient transfer learning for nlp,
571 2019. URL <https://arxiv.org/abs/1902.00751>.
- 572
- 573 Edward J. Hu, Yelong Shen, Phillip Wallis, Zeyuan Allen-Zhu, Yuanzhi Li, Shean Wang, Lu Wang,
574 and Weizhu Chen. Lora: Low-rank adaptation of large language models, 2021. URL <https://arxiv.org/abs/2106.09685>.
- 575
- 576 Yangsibo Huang, Daogao Liu, Zexuan Zhong, Weijia Shi, and Yin Tat Lee. k nn-adapter: Efficient
577 domain adaptation for black-box language models. *arXiv preprint arXiv:2302.10879*, 2023.
- 578
- 579 Albert Q Jiang, Alexandre Sablayrolles, Arthur Mensch, Chris Bamford, Devendra Singh Chaplot,
580 Diego de las Casas, Florian Bressand, Gianna Lengyel, Guillaume Lample, Lucile Saulnier, et al.
Mistral 7b. *arXiv preprint arXiv:2310.06825*, 2023.
- 581
- 582 Ariel N. Lee, Cole J. Hunter, and Nataniel Ruiz. Platypus: Quick, cheap, and powerful refinement
583 of llms. 2023.
- 584
- 585 Brian Lester, Rami Al-Rfou, and Noah Constant. The power of scale for parameter-efficient prompt
586 tuning, 2021. URL <https://arxiv.org/abs/2104.08691>.
- 587
- 588 Xiang Lisa Li and Percy Liang. Prefix-tuning: Optimizing continuous prompts for generation, 2021.
589 URL <https://arxiv.org/abs/2101.00190>.
- 590
- 591 Wing Lian, Bley Goodson, Eugene Pentland, Austin Cook, Chanvichet Vong, and "Teknium".
592 Openorca: An open dataset of gpt augmented flan reasoning traces. <https://huggingface.co/Open-Orca/OpenOrca>, 2023a.
- 593
- 594 Wing Lian, Guan Wang, Bley Goodson, Eugene Pentland, Austin Cook, Chanvichet Vong, and
595 "Teknium". Slimorca: An open dataset of gpt-4 augmented flan reasoning traces, with verifica-
596 tion, 2023b. URL <https://huggingface.co/Open-Orca/SlimOrca>.

- 594 Zhaojiang Lin, Andrea Madotto, and Pascale Fung. Exploring versatile generative language model
595 via parameter-efficient transfer learning, 2020. URL [https://arxiv.org/abs/2004.](https://arxiv.org/abs/2004.03829)
596 03829.
- 597 Alisa Liu, Xiaochuang Han, Yizhong Wang, Yulia Tsvetkov, Yejin Choi, and Noah A Smith. Tuning
598 language models by proxy. *arXiv preprint arXiv:2401.08565*, 2024.
- 600 Haokun Liu, Derek Tam, Mohammed Muqeeth, Jay Mohta, Tenghao Huang, Mohit Bansal, and
601 Colin A Raffel. Few-shot parameter-efficient fine-tuning is better and cheaper than in-context
602 learning. *Advances in Neural Information Processing Systems*, 35:1950–1965, 2022.
- 603 Ximing Lu, Faeze Brahman, Peter West, Jaehun Jung, Khyathi Chandu, Abhilasha Ravichan-
604 der, Prithviraj Ammanabrolu, Liwei Jiang, Sahana Ramnath, Nouha Dziri, Jillian Fisher, Bill
605 Lin, Skyler Hallinan, Lianhui Qin, Xiang Ren, Sean Welleck, and Yejin Choi. Inference-time
606 policy adapters (IPA): Tailoring extreme-scale LMs without fine-tuning. In Houda Bouamor,
607 Juan Pino, and Kalika Bali (eds.), *Proceedings of the 2023 Conference on Empirical Meth-*
608 *ods in Natural Language Processing*, pp. 6863–6883, Singapore, December 2023. Associa-
609 tion for Computational Linguistics. doi: 10.18653/v1/2023.emnlp-main.424. URL [https:](https://aclanthology.org/2023.emnlp-main.424)
610 [://aclanthology.org/2023.emnlp-main.424](https://aclanthology.org/2023.emnlp-main.424).
- 611 Gen Luo, Minglang Huang, Yiyi Zhou, Xiaoshuai Sun, Guannan Jiang, Zhiyu Wang, and Rongrong
612 Ji. Towards efficient visual adaption via structural re-parameterization, 2023. URL [https:](https://arxiv.org/abs/2302.08106)
613 [://arxiv.org/abs/2302.08106](https://arxiv.org/abs/2302.08106).
- 615 Rabeeh Karimi Mahabadi, James Henderson, and Sebastian Ruder. Compacter: Efficient low-rank
616 hypercomplex adapter layers, 2021. URL <https://arxiv.org/abs/2106.04647>.
- 617 Sewon Min, Mike Lewis, Luke Zettlemoyer, and Hannaneh Hajishirzi. Metaicl: Learning to learn
618 in context. *arXiv preprint arXiv:2110.15943*, 2021.
- 620 OpenAI. Chatgpt: Optimizing language models for dialogue. *OpenAI Blog*, 2022. URL [https:](https://openai.com/research/chatgpt)
621 [://openai.com/research/chatgpt](https://openai.com/research/chatgpt).
- 622 Aitor Ormazabal, Mikel Artetxe, and Eneko Agirre. CombLM: Adapting black-box language
623 models through small fine-tuned models. In Houda Bouamor, Juan Pino, and Kalika Bali
624 (eds.), *Proceedings of the 2023 Conference on Empirical Methods in Natural Language Pro-*
625 *cessing*, pp. 2961–2974, Singapore, December 2023. Association for Computational Linguis-
626 tics. doi: 10.18653/v1/2023.emnlp-main.180. URL [https://aclanthology.org/2023.](https://aclanthology.org/2023.emnlp-main.180)
627 [emnlp-main.180](https://aclanthology.org/2023.emnlp-main.180).
- 628 Long Ouyang, Jeffrey Wu, Xu Jiang, Diogo Almeida, Carroll Wainwright, Pamela Mishkin, Chong
629 Zhang, Sandhini Agarwal, Katarina Slama, Alex Ray, et al. Training language models to fol-
630 low instructions with human feedback. *Advances in neural information processing systems*, 35:
631 27730–27744, 2022.
- 633 Baolin Peng, Chunyuan Li, Pengcheng He, Michel Galley, and Jianfeng Gao. Instruction tuning
634 with gpt-4. *arXiv preprint arXiv:2304.03277*, 2023.
- 635 Jonas Pfeiffer, Andreas Rücklé, Clifton Poth, Aishwarya Kamath, Ivan Vulić, Sebastian Ruder,
636 Kyunghyun Cho, and Iryna Gurevych. Adapterhub: A framework for adapting transformers,
637 2020. URL <https://arxiv.org/abs/2007.07779>.
- 638 Xipeng Qiu, Tianxiang Sun, Yige Xu, Yunfan Shao, Ning Dai, and Xuanjing Huang. Pre-trained
639 models for natural language processing: A survey. *Science China technological sciences*, 63(10):
640 1872–1897, 2020.
- 642 Colin Raffel, Noam Shazeer, Adam Roberts, Katherine Lee, Sharan Narang, Michael Matena, Yanqi
643 Zhou, Wei Li, and Peter J Liu. Exploring the limits of transfer learning with a unified text-to-text
644 transformer. *Journal of machine learning research*, 21(140):1–67, 2020.
- 645 Colin Raffel, Noam Shazeer, Adam Roberts, Katherine Lee, Sharan Narang, Michael Matena, Yanqi
646 Zhou, Wei Li, and Peter J. Liu. Exploring the limits of transfer learning with a unified text-to-text
647 transformer, 2023. URL <https://arxiv.org/abs/1910.10683>.

- 648 Pranav Rajpurkar, Jian Zhang, Konstantin Lopyrev, and Percy Liang. Squad: 100,000+ questions
649 for machine comprehension of text, 2016. URL <https://arxiv.org/abs/1606.05250>.
650
- 651 Keisuke Sakaguchi, Ronan Le Bras, Chandra Bhagavatula, and Yejin Choi. Winogrande: An adver-
652 sarial winograd schema challenge at scale. *Communications of the ACM*, 64(9):99–106, 2021.
- 653 Haotian Sun, Yuchen Zhuang, Wei Wei, Chao Zhang, and Bo Dai. Bbox-adapter: Lightweight
654 adapting for black-box large language models. *arXiv preprint arXiv:2402.08219*, 2024.
655
- 656 Tianxiang Sun, Yunfan Shao, Hong Qian, Xuanjing Huang, and Xipeng Qiu. Black-box tuning
657 for language-model-as-a-service. In *International Conference on Machine Learning*, pp. 20841–
658 20855. PMLR, 2022.
- 659 Gemini Team, Rohan Anil, Sebastian Borgeaud, Yonghui Wu, Jean-Baptiste Alayrac, Jiahui Yu,
660 Radu Soricut, Johan Schalkwyk, Andrew M Dai, Anja Hauth, et al. Gemini: a family of highly
661 capable multimodal models. *arXiv preprint arXiv:2312.11805*, 2023.
662
- 663 Gemma Team, Morgane Riviere, Shreya Pathak, Pier Giuseppe Sessa, Cassidy Hardin, Surya Bhu-
664 patiraju, Léonard Hussenot, Thomas Mesnard, Bobak Shahriari, Alexandre Ramé, et al. Gemma
665 2: Improving open language models at a practical size. *arXiv preprint arXiv:2408.00118*, 2024.
- 666 Hugo Touvron, Louis Martin, Kevin Stone, Peter Albert, Amjad Almahairi, Yasmine Babaei, Niko-
667 lay Bashlykov, Soumya Batra, Prajjwal Bhargava, Shruti Bhosale, et al. Llama 2: Open founda-
668 tion and fine-tuned chat models. *arXiv preprint arXiv:2307.09288*, 2023.
- 669 Ashish Vaswani, Noam Shazeer, Niki Parmar, Jakob Uszkoreit, Llion Jones, Aidan N. Gomez,
670 Lukasz Kaiser, and Illia Polosukhin. Attention is all you need, 2023. URL <https://arxiv.org/abs/1706.03762>.
671
- 672 Alex Wang. Glue: A multi-task benchmark and analysis platform for natural language understand-
673 ing. *arXiv preprint arXiv:1804.07461*, 2018.
674
- 675 Alex Wang, Yada Pruksachatkun, Nikita Nangia, Amanpreet Singh, Julian Michael, Felix Hill, Omer
676 Levy, and Samuel Bowman. Superglue: A stickier benchmark for general-purpose language
677 understanding systems. *Advances in neural information processing systems*, 32, 2019.
678
- 679 Yizhong Wang, Yeganeh Kordi, Swaroop Mishra, Alisa Liu, Noah A Smith, Daniel Khashabi, and
680 Hannaneh Hajishirzi. Self-instruct: Aligning language models with self-generated instructions.
681 *arXiv preprint arXiv:2212.10560*, 2022a.
- 682 Yizhong Wang, Swaroop Mishra, Pegah Alipoormolabashi, Yeganeh Kordi, Amirreza Mirzaei, An-
683 jana Arunkumar, Arjun Ashok, Arut Selvan Dhanasekaran, Atharva Naik, David Stap, et al.
684 Super-naturalinstructions: Generalization via declarative instructions on 1600+ nlp tasks. *arXiv*
685 *preprint arXiv:2204.07705*, 2022b.
- 686 Jason Wei, Maarten Bosma, Vincent Y Zhao, Kelvin Guu, Adams Wei Yu, Brian Lester, Nan Du,
687 Andrew M Dai, and Quoc V Le. Finetuned language models are zero-shot learners. *arXiv preprint*
688 *arXiv:2109.01652*, 2021.
689
- 690 Jingqing Zhang, Yao Zhao, Mohammad Saleh, and Peter J. Liu. Pegasus: Pre-training with ex-
691 tracted gap-sentences for abstractive summarization, 2020. URL <https://arxiv.org/abs/1912.08777>.
692
- 693
694
695
696
697
698
699
700
701

APPENDIX

A ANALYSIS OF MODEL PERFORMANCE UNDER MULTIPLE CONTINUAL UPDATES

To validate our framework’s robustness under periodic updates, we conducted experiments simulating multiple rounds of continued pretraining. Using `Mistral-7B` as our base model, we performed four sequential updates using different pretraining datasets: `OpenOrca` \rightarrow `OpenPlatypus` \rightarrow `Alpaca` \rightarrow `GPT4-LLM-Cleaned`. For the hyperparameters we utilize the same settings described in Section 4. We evaluated our model patch on all seven downstream tasks after each update. The results are summarized in Table A. Our experiments yield the following key findings:

Time	Model Version	BoolQ	SST-2	MRPC	RTE	WinoGrande	WNLI	GSM8K
		Accuracy	Accuracy	Accuracy/F1	Accuracy	Accuracy	Accuracy	Accuracy
$T = 0$	Pretrained Model θ	83.58	66.86	65.20 / 73.70	67.51	74.11	57.76	6.37
	None	91.01	95.99	89.46 / 92.62	87.73	85.95	83.11	34.04
$T = 1$	Updated Model θ'	87.46	82.91	74.75 / 83.73	75.09	75.06	57.72	15.16
	Ours $\theta' + \Delta\theta_i$	90.24	96.11	88.73 / 92.10	89.17	85.01	83.10	41.32
$T = 2$	Updated Model θ'	86.33	86.81	76.23 / 83.53	71.48	74.51	52.11	12.36
	OpenPlatypus	89.88	96.22	88.24 / 91.55	88.09	84.37	83.10	42.15
$T = 3$:	Updated Model θ'	87.03	85.78	74.02 / 83.33	73.65	74.27	56.34	16.38
	Alpaca	89.66	96.33	88.73 / 92.12	88.81	85.08	83.10	38.21
$T = 4$:	Updated Model θ'	85.11	75.79	72.78 / 82.79	74.37	71.67	56.34	14.94
	GPT4-LLM	88.41	96.10	87.01 / 90.91	85.56	80.19	77.46	31.77

Table A: Model performance across sequential updates ($T=0$ to $T=4$) on seven downstream tasks. We report accuracy for all tasks except MRPC, where we show both accuracy and F1 score.

① Across all update stages ($T = 0$ to $T = 4$), applying our model patches results in substantial zero-shot improvements over the updated model θ' . These improvements are consistent and significant across different tasks, with SST-2 showing gains from +9.41% to +20.31%, WNLI maintaining strong improvements between +21.12% and +30.99%, and MRPC consistently improving by +12 – 14% in accuracy. Notably, these improvements are achieved without any additional training, requiring only a simple merge operation of our model patches.

② The performance stability of our patched models is particularly noteworthy when compared to the fluctuating zero-shot performance of θ' . As shown in Table A, our method maintains remarkably consistent performance across multiple updates. For instance, BoolQ accuracy remains within a tight range of 88.41 – 90.24%, SST-2 consistently maintains accuracy above 96%, and MRPC’s F1 score stays above 90 across all update stages. These results demonstrate our method’s robustness to successive model updates and its ability to preserve task-specific knowledge.

③ Furthermore, our method shows interesting behavior in leveraging complementary knowledge from different updates. Taking GSM8K as an example, we observe varying but significant improvements ranging from +16.83% to +29.79% across different update stages. This suggests that our model patches can effectively combine knowledge from both the original fine-tuning and the continued pretraining updates, sometimes leading to performance gains that exceed what might be expected from either source alone. Such behavior demonstrates the potential of our approach to not just preserve but potentially enhance task performance through knowledge integration across model versions.

B ANALYSIS OF LORA RANK SELECTION FOR DOWNSTREAM TASKS

To validate our choice of LoRA rank and understand its impact on model performance, we conducted experiments with varying ranks. This analysis helps establish the optimal balance between computational efficiency and model effectiveness. To perform these experiments we utilize `Mistral-7B` with `OpenOrca` as the continued pretraining dataset, and evaluate on BoolQ, MRPC, WNLI downstream tasks with a varying rank for LoRA. Rest of the hyper-parameters are the same as in Section 4. The results can be seen in Table B.

① Both fine-tuning θ_i and our method $\theta' + \Delta\theta_i$ demonstrate remarkable stability across different ranks, with optimal performance typically achieved at rank 8-16. Specifically, on BoolQ, we observe peak accuracy at rank 16, while MRPC and WNLI show optimal performance at rank 8. This consistency across ranks validates the robustness of our approach and suggests that model patches effectively capture task-specific knowledge regardless of rank selection.

② When examining the efficiency aspects, we find that increasing rank beyond 8 provides diminishing or even negative returns. As shown in Table B, at rank 32, we observe decreased performance across most tasks compared to rank 8: BoolQ drops by 1.01%, MRPC by 0.49%, and WNLI by 2.83%. Importantly, the performance gap between our method and direct fine-tuning remains minimal even at lower ranks, with differences of less than 1% in most cases. This suggests that our training-free approach maintains its effectiveness even with more constrained rank settings.

③ Our analysis strongly justifies our original choice of rank 8 as the default setting. This configuration achieves an optimal balance between computational efficiency (requiring fewer parameters than higher ranks), model performance (maintaining competitive results across all tasks), and adaptation capability (providing sufficient capacity for task-specific learning). Notably, while higher ranks like 16 or 32 require significantly more parameters, they offer minimal or no performance benefits, making rank 8 the sweet spot for our training-free framework.

Rank	Model Version	BoolQ Accuracy	MRPC Accuracy/F1	WNLI Accuracy
$r = 2$	Fine-tuned Model θ_i	90.52	87.30 / 91.28	74.65
	Ours $\theta' + \Delta\theta_i$	89.85	87.01 / 91.03	77.46
$r = 4$	Fine-tuned Model θ_i	90.81	89.42 / 91.98	78.23
	Ours $\theta' + \Delta\theta_i$	90.18	87.75 / 91.53	80.28
$r = 8$	Fine-tuned Model θ_i	91.01	89.46 / 92.62	83.11
	Ours $\theta' + \Delta\theta_i$	90.24	88.73 / 92.10	83.10
$r = 16$	Fine-tuned Model θ_i	91.07	89.22 / 92.49	81.69
	Ours $\theta' + \Delta\theta_i$	90.98	88.97 / 92.31	82.98
$r = 32$	Fine-tuned Model θ_i	90.00	88.97 / 92.15	80.28
	Ours $\theta' + \Delta\theta_i$	90.28	88.73 / 91.93	81.69

Table B: Performance comparison across different LoRA ranks (2, 4, 8, 16, 32) on three downstream tasks using Mistral-7B.

C PROOF OF LEMMA 1

Notations: $\mathcal{C}(\cdot)$ returns the column vector subspace of a matrix.

Recall in Section 3.3, we decomposed the fine-tuned updated model θ'_i into two terms:

$$\theta'_i = \theta' + \Delta\theta'_i \tag{8a}$$

$$= \underbrace{(\theta' + \Delta\theta_i)}_{\text{Naive Update } \hat{\theta}'_i} + \underbrace{(\Delta\theta'_i - \Delta\theta_i)}_{\text{Residual Matrix } R}. \tag{8b}$$

Lemma 1: The residual matrix R is negligible compared to the naive update $\hat{\theta}'_i$ in terms of the Frobenius norm.

810 *Proof:* Our goal is to show that the error ratio $\|R\|_F^2 / \|\hat{\theta}'_i\|_F^2$ is small. We will proceed by finding a
 811 large enough numerator $\|R\|_F^2$ and small enough $\|\hat{\theta}'_i\|_F^2$ in the LoRA context and show that the upper
 812 bound of the error ratio is small.
 813
 814

815 **Numerator** $\|R\|_F^2$. First, we search for conditions that potentially lead to residual matrices with
 816 larger Frobenius norm. We apply compact SVD to the patches $\Delta\theta_i$ and $\Delta\theta'_i$ designating subscripts
 817 1 and 2 for SVD matrices, respectively:

$$818 \quad \|R\|_F^2 = \|\Delta\theta'_i - \Delta\theta_i\|_F^2 \quad (9a)$$

$$819 \quad = \|U_2 \Sigma_2 V_2^T - U_1 \Sigma_1 V_1^T\|_F^2 \quad (9b)$$

$$820 \quad = \left\| \sum_{\ell=1}^{r_2} \sigma_\ell^{(2)} u_\ell^{(2)} v_\ell^{(2)T} - \sum_{k=1}^{r_1} \sigma_k^{(1)} u_k^{(1)} v_k^{(1)T} \right\|_F^2. \quad (9c)$$

821 Here, the typical order of magnitude for r_1 and r_2 is about 10.

822 1. When there is no intersection between the two pairs of singular vector subspaces, namely, $\mathcal{C}(U_1) \cap$
 823 $\mathcal{C}(U_2) = \emptyset$ and $\mathcal{C}(V_1) \cap \mathcal{C}(V_2) = \emptyset$, the two terms in (9c) may be combined to form a valid compact
 824 SVD of rank $r_1 + r_2$ as follows:

$$825 \quad \|R\|_F^2 = \left\| \sum_{\ell=1}^{r_2} \sigma_\ell^{(2)} u_\ell^{(2)} v_\ell^{(2)T} + \sum_{k=1}^{r_1} \sigma_k^{(1)} \cdot (-u_k^{(1)}) v_k^{(1)T} \right\|_F^2 \quad (10a)$$

$$826 \quad = \left\| \sum_{k'=1}^{r_1+r_2} \sigma_{k'}^{(1,2)} u_{k'}^{(1,2)} v_{k'}^{(1,2)T} \right\|_F^2, \quad (10b)$$

827 where $\sigma_1^{(1,2)}, \dots, \sigma_{r_1+r_2}^{(1,2)}$ is a list of descending ordered positive numbers sampled without replace-
 828 ment from $\{\sigma_k^{(1)}\}_{k=1}^{r_1}$ and $\{\sigma_\ell^{(2)}\}_{\ell=1}^{r_2}$. Applying the Frobenius norm property to the SVD represen-
 829 tation of a matrix, we obtain

$$830 \quad \|R\|_F^2 = \sum_{k'=1}^{r_1+r_2} [\sigma_{k'}^{(1,2)}]^2 = \sum_{\ell=1}^{r_2} [\sigma_\ell^{(2)}]^2 + \sum_{k=1}^{r_1} [\sigma_k^{(1)}]^2. \quad (11)$$

831 This is the case when the two patches $\Delta\theta_i$ and $\Delta\theta'_i$ contain only orthogonal information. This is not
 832 very realistic, because the two patches were created on the same downstream task i that should lead
 833 to some information in common.
 834

835 2. When the two patches have are oppositely embedded in one of the singular value subspaces, e.g.,
 836 $U_2 = -U_1$ and $V_2 = V_1$, the two terms in (9c) can be merged and singular values with the same
 837 ranking will be summed up, namely,

$$838 \quad \|R\|_F^2 = \left\| \sum_{\ell=1}^{r_2} \sigma_\ell^{(2)} u_\ell^{(2)} v_\ell^{(2)} + \sum_{k=1}^{r_1} \sigma_k^{(1)} \cdot (-u_k^{(1)}) v_k^{(1)T} \right\|_F^2 \quad (12a)$$

$$839 \quad = \left\| \sum_{\ell=1}^{r_2} [\sigma_\ell^{(2)} + \sigma_\ell^{(1)}] u_\ell^{(2)} v_\ell^{(2)} \right\|_F^2 \quad (12b)$$

$$840 \quad = \sum_{\ell=1}^{r_2} [\sigma_\ell^{(2)} + \sigma_\ell^{(1)}]^2, \quad (12c)$$

841 which can be easily shown that it is larger than the orthogonal case (11) due to the extra interaction
 842 term $\sum_{\ell=1}^{r_2} \sigma_\ell^{(2)} \sigma_\ell^{(1)}$. When $\sigma_\ell^{(2)} = \sigma_\ell^{(1)}$, this case corresponds to two patches having exactly oppo-
 843 site gradient update directions, which again is not very realistic because the same downstream tasks

are used to generate the update directions. Equations (11) and (12c) both correspond to extreme conditions, and the continuum in between should be more realistic. We will use the large numerator (12c) to examine the error ratio.

Denominator $\left\| \hat{\theta}'_i \right\|_F^2$. We continue to apply compact SVD to the continued pretrained model θ' and patch $\Delta\theta_i$ designating subscripts 0 and 1 for SVD matrices, respectively:

$$\left\| \hat{\theta}'_i \right\|_F^2 = \left\| \theta' + \Delta\theta_i \right\|_F^2 \quad (13a)$$

$$= \left\| U_0 \Sigma_0 V_0^T + U_1 \Sigma_1 V_1^T \right\|_F^2 \quad (13b)$$

$$= \left\| \sum_{j=1}^{r_0} \sigma_j^{(0)} u_j^{(0)} v_j^{(0)T} + \sum_{k=1}^{r_1} \sigma_k^{(1)} u_k^{(1)} v_k^{(1)T} \right\|_F^2. \quad (13c)$$

Here, the typical order of magnitude for r_0 is about 100. 1. When there is no intersection between the two pairs of singular vector subspaces, the two terms may be combined to form a valid compact SVD of rank $r_0 + r_1$. Hence, similar to (11), we have

$$\left\| \hat{\theta}'_i \right\|_F^2 = \sum_{j=1}^{r_0} \left[\sigma_j^{(0)} \right]^2 + \sum_{k=1}^{r_1} \left[\sigma_k^{(1)} \right]^2. \quad (14)$$

2. When the basis vectors of singular matrices (with one matrix having opposite signs) of the patch can be found in the singular matrices of the continued pretrained model, we are able to combine the two terms in (13c) by using the basis vectors of U_0 and V_0 as follows:

$$\left\| \hat{\theta}'_i \right\|_F^2 = \left\| \sum_{j=1}^{r_0} \sigma_j^{(0)} u_j^{(0)} v_j^{(0)T} + \sum_{j=1}^{r_0} \sigma_j^{(1')} u_j^{(0)} v_j^{(0)T} \right\|_F^2, \quad (15a)$$

$$= \sum_{j=1}^{r_0} \left[\sigma_j^{(0)} - \sigma_j^{(1')} \right]^2, \quad (15b)$$

where we define an auxiliary symbol

$$\sigma_j^{(1')} = \begin{cases} \sigma_k^{(1)}, & \exists k \in [1, r_1] \text{ s.t. } u_j^{(0)} = u_k^{(1)}, \\ 0, & \text{other } k. \end{cases} \quad (16)$$

Both (14) and (15b) correspond to the extreme cases. Since (15b) leads to a smaller denominator, we will use it to examine the error ratio.

Error Ratio. Using (12c) and (15b), a pessimistic error ratio can be approximated and then up bounded as follows:

$$\frac{\|R\|_F^2}{\left\| \hat{\theta}'_i \right\|_F^2} \approx \frac{\sum_{\ell=1}^{r_2} \left[\sigma_\ell^{(2)} + \sigma_\ell^{(1)} \right]^2}{\sum_{j=1}^{r_0} \left[\sigma_j^{(0)} - \sigma_j^{(1')} \right]^2} \quad (17a)$$

$$\leq \frac{r_2 \cdot \max_\ell \left[\sigma_\ell^{(2)} + \sigma_\ell^{(1)} \right]^2}{r_0 \cdot \min_j \left[\sigma_j^{(0)} - \sigma_j^{(1')} \right]^2} \quad (17b)$$

$$= \frac{r_2}{r_0} \cdot \nu, \quad (17c)$$

where $\nu = \max_\ell \left[\sigma_\ell^{(2)} + \sigma_\ell^{(1)} \right]^2 / \min_j \left[\sigma_j^{(0)} - \sigma_j^{(1')} \right]^2$ is a singular-value based constant. Given that the rank r_2 of the patch is at least one order of magnitude smaller than the rank r_0 of the pretrained model, we conclude residual matrix term is negligible compared to the naive update term.